# Aromaticity in Group 14 Metalloles: Structural, Energetic, and Magnetic Criteria

Bernd Goldfuss and Paul von Ragué Schleyer*

*Institut für Organische Chemie der Universität Erlangen-Nürnberg, Henkestrasse 42, D-91054 Erlangen, Germany*

*Received November 25, 1996*[⊗]

Various structural (C−C bond length equalization, *D*), energetic (isodesmic stabilization energies, ISE), and magnetic (diamagnetic susceptibility exaltations, Λ and nucleus-independent chemical shifts, NICS) criteria are employed (using B3LYP, CSGT, and GIAO *ab initio* methods) to assess the aromaticity and antiaromaticity of a variety of group 14 (E = C, Si, Ge, Sn, Pb) metalloles: $C_4H_4EH_2$ ($C_{2v}$), $C_4H_4EH^-$ ($C_s$ and $C_{2v}$; C, $D_{5h}$), $C_4H_4EH^+$ (singlet, $C_{2v}$), $C_4H_4EHLi$ ($C_s$; C, $C_{5v}$), and $C_4H_4ELi_2$ ($C_{2v}$). In addition, structural trends are established for $C_4H_4ELi^-$ ($C_s$) and for $C_4H_4E^{2-}$ ($C_{2v}$) as well as for the singlet and triplet $C_4H_4E$ ($C_{2v}$) sets. The increased pyramidality at E down group 14 results in strongly decreased aromaticity of metallolyl anions $C_4H_4EH^-$ ($C_s$). In contrast, all planar $C_4H_4EH^-$ ($C_{2v}$) geometries are significantly more aromatic. Although all $C_4H_4EH^+$ ($C_{2v}$) structures are planar, the antiaromaticity in singlet $C_5H_5^+$ is much higher than that of the heavier congeners (E = Si to Pb). The four-$\pi$-electron singlets $C_4H_4E$ exhibit nearly as localized geometries as the $C_4H_4EH^+$ ions, but the $C_4H_4E$ triplets are more delocalized. As in the free anions, pyramidally coordinated E's lead in $C_4H_4EHLi$ ($C_s$) to reduced aromaticity, but stabilizing Li−H interactions are apparent in these structures. The metallole dianions and their $Li^+$ complexes (e.g. $C_4H_4ELi_2$, $C_{2v}$) are the most aromatic among the species studied. The aromaticity in these dianionic metalloles is remarkably constant in going from E = C to E = Pb.



## Introduction

The substantial aromaticity of the cyclopentadienyl anion and of many six-$\pi$-electron $C_4H_4E$ heterocycles[1] (e.g. pyrrole and thiophene)[2] has inspired a search for group 14 congeners (E = $SiH^-$ to $PbH^-$).[3] The lower degree of conjugation and aromaticity in $C_4H_4E$ ($C_s$, E = $SiH^-$, PH) relative to their second-period congeners ($C_{2v}$, E = $CH^-$, NH) is due to the pyramidal environments at the heteroatoms.[4] The pyramidalization problem does not arise when divalent second-row groups are involved, e.g. in thiophene and the phospholyl anion.[5]

The results of early studies on metallole anions were frustrating; "despite considerable effort no silaaromatic compounds have yet been isolated"[6] and "attempts to confirm the aromaticity of germolyl anions by $\eta^5$-coordination to transition metals have been unsuccessful".[7] However, progress in metallole chemistry now has improved this situation dramatically.

Freeman et al. first established the $\eta^5$-coordination of germolyl (**1**)[8] and of silolyl (**2**, **3**)[9] moieties in Ru complexes by X-ray crystal diffraction and NMR studies. The analogy to $\eta^5$-cyclopentadienides in transition-metal complexes is apparent.

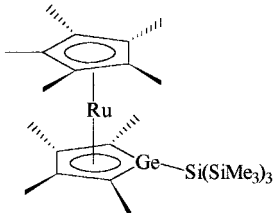


**1**

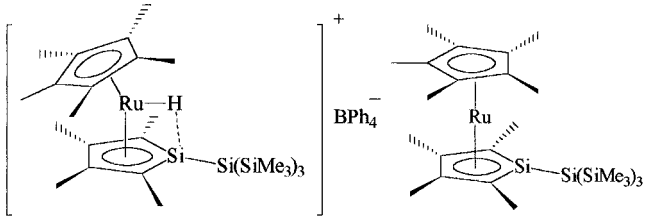


**2** **3**

Based on the upfield $\delta(^{13}C_{\alpha,\beta})$ and downfield $\delta(^{29}Si)$ chemical shifts, Hong and Boudjouk suggested that **4** was delocalized and aromatic.[10] However, earlier $\delta(^1H)$

[⊗] Abstract published in *Advance ACS Abstracts,* March 15, 1997.

(1) Minkin, V. I.; Glukhovtsev, M. N.; Simkin, B. Y. *Aromaticity and Antiaromaticity*; Wiley: New York, 1994.

(2) (a) Schleyer, P. v. R.; Freeman, P. K.; Jiao, H.; Goldfuss, B. *Angew. Chem.* **1995**, *107*, 332; *Angew. Chem., Int. Ed. Engl.* **1995**, *34*, 337. (b) Grützmacher, H.; *Angew. Chem.* **1995**, *107*, 323; *Angew. Chem., Int. Ed. Engl.* **1995**, *34*, 295. (c) Schleyer, P. v. R.; Jiao, H. *Pure Appl. Chem.* **1996**, *68*, 209. (d) Schleyer, P. v. R.; Kapp, Y.; Jiao, H.; Goldfuss, B.; Maerker, C.; Korkin, A.; Subramanian, G.; Hommes, N. V. E. XIth International Symposium on Organosilicon Chemistry, Montpellier, France, September 1−6, 1996.

(3) See refs 6 and 7 and: (a) Kapp, J.; Schleyer, P. v. R. In *The Chemistry of Organic Silicon Compounds*; Patai, S., Ed.; in press. (b) Nagase, S.; Sekiguchi, A. In *The Chemistry of Organic Silicon Compounds*; in press. (c) Driess, M.; Grützmacher, H. *Angew. Chem.* **1996**, *108*, 900; *Angew. Chem., Int. Ed. Engl.* **1996**, *35*, 828. (d) Jemmis, E. D.; Srinivas, G. N.; Leszczynki, J.; Kapp, J.; Korkin, A. A.; Schleyer, P. v. R. *J. Am. Chem. Soc.* **1995**, *117*, 11361. (e) Kapp, J.; Remko, M.; Schleyer, P. v. R. *J. Am. Chem. Soc.* **1996**, *118*, 5745. (f) Gobbi, A.; Frenking, G. *J. Am. Chem. Soc.* **1994**, *116*, 9287.

(4) (a) Kutzelnigg, W. *Angew. Chem.* **1984**, *96*, 262; *Angew. Chem., Int. Ed. Engl.* **1984**, *23*, 272. (b) Kapp, Y.; Schade, C.; El-Nahas, A.; Schleyer, P. v. R. *Angew. Chem.* **1996**, *108*, 2373; *Angew. Chem., Int. Ed. Engl.* **1996**, *35*, 2236.

(5) (a) Glukhovtsev, M. N.; Dransfeld, A.; Schleyer, P. v. R. *J. Phys. Chem.* **1996**, *100*, 13447. (b) Glukhovtsev, M. N.; Schleyer, P. v. R.; Maerker, C. *J. Phys. Chem.* **1993**, *97*, 8200.

(6) Apeloig, Y. In *The Chemistry of Organic Silicon Compounds*; Patai, S., Rappoport, Z., Eds.; Wiley: Chichester, U.K., 1989; p 151 and references therein.

(7) Colmer, E.; Corriu, R. J. P.; Lheureux, M. *Chem. Rev.* **1990**, *90*, 265 and references therein.

S0276-7333(96)00994-6 CCC: $14.00 

($CH_3$) NMR data on the methyl derivative **5** were considered to be consistent with a high negative charge on Si rather than significant charge delocalization.[11] Likewise, Dufour et al. concluded from the deshielded $\delta(^{13}C_{\alpha,\beta})$ value in **6** that "the negative charge is localized on the germanium atom".[12]

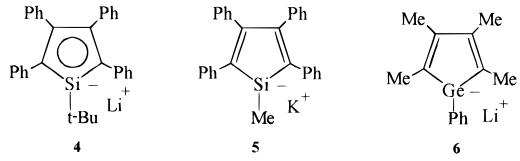


**4** **5** **6**

In view of such different conclusions, we have undertaken a comprehensive analysis of metallole aromaticity. We employed structural, energetic, and magnetic criteria for aromaticity to assess the aromaticity and antiaromaticity of a large set of five-membered-ring heterocycles.[2] Using the same methods, significant aromatic character was found for the parent silolyl anion $C_4H_4SiH^-$ (**7**, $C_{2v}$; **8**, $C_s$; MP2/6-31+G**),[13] in contrast to earlier studies at lower theoretical levels.[14] The aromaticity of **8** is enhanced by $\eta^5$-$Li^+$ complexation in $C_4H_4SiHLi$ (**9**).[13]

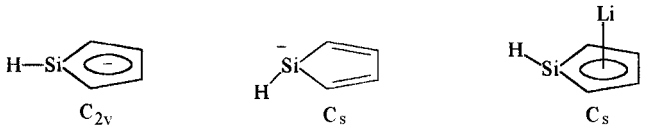


**7** **8** **9**

Freeman et al.'s X-ray crystal structure of the counterion-separated germolyl anion **10** showed localized C−C bonds ($C_\alpha-C_\beta$ = 1.36 Å, $C_\beta-C_\beta$ = 1.46 Å) and a pyramidal Ge (angle sum 281°) environment.[15] However, Ru $\eta^5$ coordination to the germolyl anion **10** resulted in a significantly more delocalized germolyl geometry in **1** ($C_\alpha-C_\beta$ = 1.42 Å, $C_\beta-C_\beta$ = 1.42 Å, angle sum at Ge 358°).[8] Similarly, increased delocalization due to counterion coordination was found computationally for $\eta^5$-$C_4H_4SiHLi$ (**9**; $C_\alpha-C_\beta$ = 1.420 Å, $C_\beta-C_\beta$ = 1.424 Å, angle sum at Si 340.2°) relative to **8** ($C_\alpha-C_\beta$ = 1.399 Å, $C_\beta-C_\beta$ = 1.433 Å, angle sum at Si = 321.6°).[13] The germolyl and silolyl moieties of **11** ($C_\alpha-C_\beta$ = 1.34 Å, $C_\beta-C_\beta$ = 1.47 Å, angle sum at Ge 295°), **12** ($C_\alpha-C_\beta$ = 1.33 Å, $C_\beta-C_\beta$ = 1.48 Å, angle sum at Ge 291°) and **13** ($C_\alpha-C_\beta$ = 1.36 Å, $C_\beta-C_\beta$ = 1.45 Å, angle sum at Ge 279°) exhibit localized C−C bonds and pyramidal ring heteroatom environments.[16]

Hong et al. synthesized and characterized the trisgermole **14**[17] and found $\eta^1$ $\sigma$(Ge) ($\delta(^7Li) = -0.9$) as well as $\eta^4/\eta^5$ $\pi$-bonded Li ions ($\delta(^7Li) = -5.0$).[18]

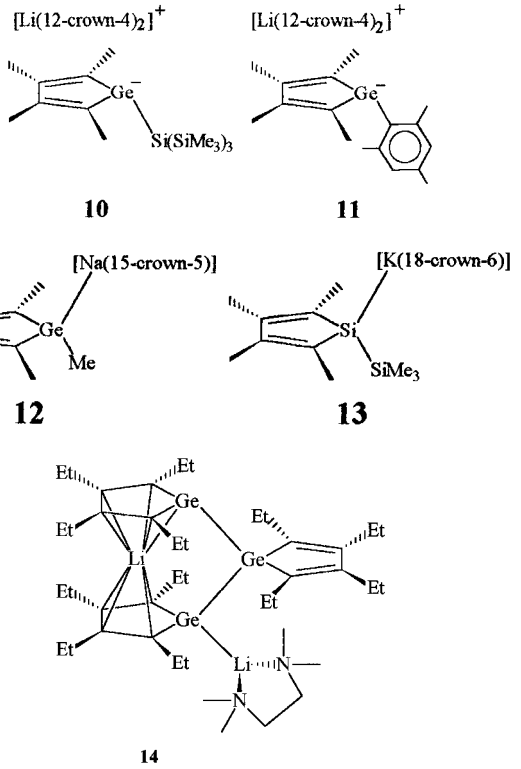


**14**

Decreased conjugation due to pyramidalization at the heteroatom is not present in metallole dianions (i.e.: $C_4H_4E^{2-}$, E = C to Pb). In 1987 Joo, Park, Kang, and Hong reported the first synthesis of a silole dianion with sodium (**16-Na**) and potassium (**16-K**) counterions.[19] Subsequently, the $^{13}C$ NMR data of **16-Na** were published[20] and the lithium derivative **16-Li** was synthesized in THF solution; the upfield $\delta(^{13}C)$ and the downfield $\delta(^{29}Si)$ displacements in **16-Li** (relative to **15**) were attributed to charge delocalization and aromaticity.[21] Indeed, our analysis of structural, energetic and magnetic criteria of the silole dianion $C_4H_4Si^{2-}$ (and its alkali-metal ion pairs) revealed a high degree of aromaticity.[22] The aromatic stabilization energy (ASE) of $\eta^5$-$C_4H_4SiLi^-$ (36.4 kcal/mol) even exceeded that of the isoelectronic phosphole $\eta^5$-$C_4H_4PLi^-$ (ASE = 34.1 kcal/mol) and thiophene $\eta^5$-$C_4H_4SLi^+$ (ASE = 27.1 kcal/mol) analogues.[22] In contrast, electron-withdrawing chlorines resulted in rather strongly alternating C−C silole distances ($C_\alpha-C_\beta$ = 1.35 Å, $C_\beta-C_\beta$ = 1.54 Å) in the X-ray crystal structure of the 1,1-dichlorosilole $C_4Ph_4SiCl_2$ (**15**), consistent with some degree of antiaromatic character.[22]

(8) Freeman, W. P.; Tilley, T. D.; Rheingold, A. L.; Ostrander, R. L. *Angew. Chem.* **1993**, *105*, 1841; *Angew. Chem., Int. Ed. Engl.* **1993**, *32*, 1744.
(9) Freeman, W. P.; Tilley, T. D.; Rheingold, A. L. *J. Am. Chem. Soc.* **1994**, *116*, 8428.
(10) Hong, J.-H.; Boudjouk, P. *J. Am. Chem. Soc.* **1993**, *115*, 5883.
(11) Han, B.-H.; Boudjouk, P. *Chungnam Kawhak Yonguchi* **1984**, *11*, 101.
(12) Dufour, P.; Dubac, J.; Dartiguenave, M.; Dartiguenave, Y. *Organometallics* **1990**, *9*, 3001.
(13) Goldfuss, B.; Schleyer, P. v. R. *Organometallics* **1995**, *14*, 1553.
(14) (a) Gordon, M. S.; Boudjouk, P.; Anwari, F. *J. Am. Chem. Soc.* **1983**, *105*, 4972. (b) Damewood, J. R. *J. Org. Chem.* **1986**, *51*, 5028.
(15) Freeman, W. P.; Tilley, T. D.; Arnold, F. P., Rheingold, A. L.; Gantzel, P. K. *Angew. Chem.* **1995**, *107*, 2029; *Angew. Chem., Int. Ed. Engl.* **1995**, *34*, 1887.
(16) Freeman, W. P.; Tilley, T. D.; Liable-Sands, L. M.; Rheingold, A. L. *J. Am. Chem. Soc.* **1996**, *118*, 10457.
(17) Hong, J.-H.; Pan, Y.; Boudjouk, P. *Angew. Chem.* **1996**, *108*, 213; *Angew. Chem., Int. Ed. Engl.* **1996**, *35*, 186.
(18) High-field $\delta(^{6,7}Li)$ values indicate aromatic ring currents; see ref 13 and: (a) Paquette, L. A.; Bauer, W.; Sivik, M. R.; Bühl, M.; Feigel, M.; Schleyer, P. v. R. *J. Am. Chem. Soc.* **1990**, *112*, 8776. (b) Jiao, H.; Schleyer, P. v. R. *Angew. Chem.* **1993**, *105*, 1830; *Angew. Chem., Int. Ed. Engl.* **1993**, *32*, 1760.
(19) Joo, W. C.; Park, Y. C.; Kang, S. K.; Hong, J.-H. *Bull. Korean Chem. Soc.* **1987**, *8*, 270.
(20) Joo, W.-C.; Hong, J.-H.; Choi, S.-B.; Son, H.-E. *J. Organomet. Chem.* **1990**, *391*, 27.
(21) (a) Hong, J.-H.; Boudjouk, P.; Castellino, S. *Organometallics* **1994**, *13*, 3387. (b) Goldfuss, B. Diplomarbeit, Erlangen, Germany, 1993. (c) Goldfuss, B. 8th International Symposium on Novel Aromatic Compounds, Braunschweig, Germany, 1995.
(22) Goldfuss, B.; Schleyer, P. v. R.; Hampel, F. *Organometallics* **1996**, *15*, 1755.

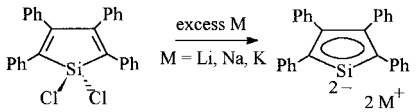


X-ray crystal structures of **16-Li** (5 THF)[23] and of **17**[24] showed $\eta^5$ alkali-metal coordinations and nearly equal C−C bond lengths ($C_\alpha-C_\beta = 1.44$ Å, $C_\beta-C_\beta = 1.43$ Å in **16-Li**; $C_\alpha-C_\beta = 1.39$ Å, $C_\beta-C_\beta = 1.44$ Å in **17**).

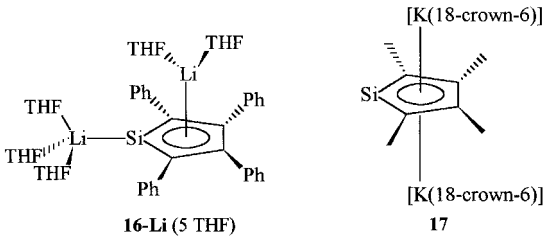


West et al. crystallized the polar dilithium germole **18** at −20 °C as a $\eta^5/\eta^5$ species and at +25 °C as $\eta^1/\eta^5$ complex.[25] Freeman et al. characterized a columnar structure of the dipotassium germole **19**.[16]

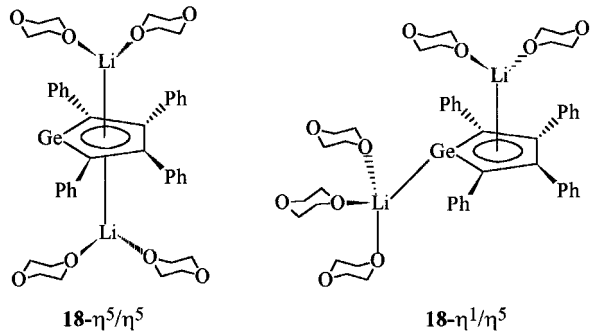


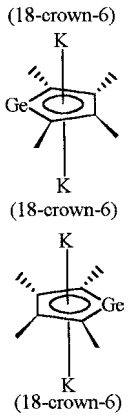


The nearly equal C−C distances in the X-ray crystal structures of **18-**$\eta^5/\eta^5$ ($C_\alpha-C_\beta = 1.43$ Å, $C_\beta-C_\beta = 1.45$ Å), of **18-**$\eta^1/\eta^5$ ($C_\alpha-C_\beta = 1.42$ Å, $C_\beta-C_\beta = 1.44$ Å), and of **19** ($C_\alpha-C_\beta = 1.43$ Å, $C_\beta-C_\beta = 1.43$ Å) point to delocalized $\pi$-systems.

**Scheme 1. Interrelationships of Metallole Structures**[a]

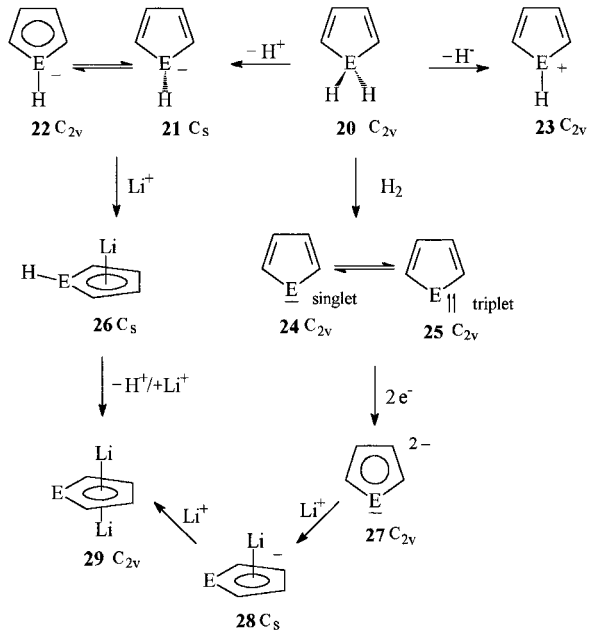


[a] E = C (except for **21**), Si, Ge, Sn, Pb. **22-C** has $D_{5h}$ symmetry, **26-C** has $C_{5v}$ symmetry, and **23-C** is a singlet.

The increasing number of such metalloles which are being reported prompts the quantitative, systematic evaluation of their aromatic character. What trends can be expected for these metalloles in going down group 14? We now compute structural, energetic and magnetic criteria to assess comprehensively the aromatic (or antiaromatic) degree in a variety of anionic and cationic group 14 metallole species (Scheme 1).

## Results and Discussion

**Structures and Energies.** Nearly equal C−C bond lengths indicate delocalized $\pi$-systems.[2,26] The degree of C−C bond equalization in the metallole rings of **20**−**29** (Figures 1−7, Chart 1, Table 1) is given most simply by the difference in the $C_\beta-C_\beta$ and $C_\alpha-C_\beta$ bond lengths, $D$.[26]

Deprotonation of 1,1-dihydrometalloles **20** decreases the C−C bond length differences, $D$, in **21** and in **22** (Figure 8). As one goes from C to Pb, the $D$'s increase (the differences in C−C bond lengths are larger) in **20**, in **21** (strongly), and in **22** (slightly; Figure 8). The C−C bond length alternation in **21** even approaches that of **20** for the heavier metalloles (E = Sn, Pb; Figure 8). Significant C−C bond length alternations and pyramidal heteroatom environments were found in the X-ray crystal structures of the anions of **10** ($D = 0.10$)[15] and of **11** ($D = 0.13$).[16]

Pyramidality at the trivalent heteroatoms (measured by the angle sums at E) in **21-Si** to **21-Pb** (Figure 2) results in decreased conjugation and larger differences in C−C bond lengths.[27] The angle sums at E correlate linearly with the D values for **21** from C to Pb (Figure 9). The more pyramidal species have the largest inver-

(23) West, R.; Sohn, H.; Bankwitz, U.; Calabrese, J.; Apeloig, Y.; Müller, T. *J. Am. Chem. Soc.* **1995**, *117*, 11608.

(24) Freeman, W. P.; Tilley, T. D.; Yap, G. P. A.; Rheingold, A. L. *Angew. Chem.* **1996**, *108*, 960; *Angew. Chem., Int. Ed. Engl.* **1996**, *35*, 882.

(25) West, R.; Sohn, H.; Powell, D. R.; Müller, T.; Apeloig, Y. *Angew. Chem.* **1996**, *108*, 1095; *Angew. Chem., Int. Ed. Engl.* **1996**, *35*, 1002.

(26) $D = (C_\beta C_\beta - C_\alpha C_\beta)$. Julg's parameter relates the bond length equalization to benzene; see refs 2, 13, 22, and: (a) Julg, A.; Francois, P. *Theor. Chim. Acta* **1967**, *7*, 249. (b) Kerk, S. M. v. d. *J. Organomet. Chem.* **1981**, *215*, 315.

(27) For a discussion of the high inversion barriers in trivalent heavy elements, see ref 4.

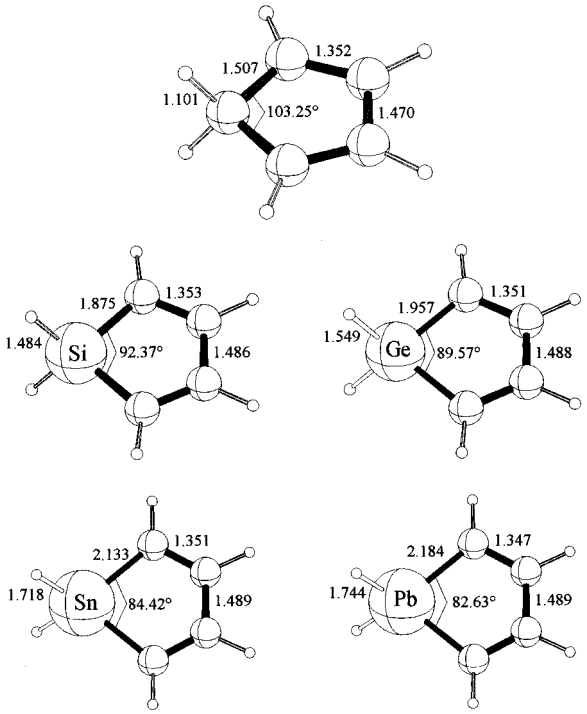


**Figure 1.** Optimized geometries (B3LYP/6-31+G* (C, H), /LanL2DZdp (E)) of 1,1-dihydrometalloles **20** ($C_{2v}$). Bond distances are given in Å.

sion barriers: the pyramidality at E and the inversion barriers (**21** → **22**) increase from C to Pb (Table 2).[28] Accordingly, inversion barriers were measured by dynamic NMR to be higher for germolyl anions than for silolyl anions: $[(C_4Et_4GeSiMe_3][Li(12\text{-crown-}4)_2]$ (10.5(1) kcal/mol), $C_4Et_4GeSiMe_3K$ (9.4(1) kcal/mol), $[C_4Et_4SiSiMe_3][Li(12\text{-crown-}4)_2]$ (< 8.4 kcal/mol), and $C_4Et_4SiSiMe_3K$ (<8.4 kcal/mol).[16]

Relative to the dimethyl derivatives **30** and **31**, the inversion barriers in the metallolyl anions **21** and **22** are reduced more strongly for Si (by 26.6 kcal/mol) and for Ge (by 25.9 kcal/mol) than for Sn (by 18.4 kcal/mol) and Pb (by 20.1 kcal/mol; Tables 2 and 3).

**30** $C_s$ **31** $C_{2v}$

E = C, Si, Ge, Sn, Pb

Both the degree of planarity at E and the EH−Li distances decrease from C to Pb in the $\eta^5$-lithium metallolides **26** (Figure 5). As in **21**, a linear correlation between the angle sums at E and the C−C bond length equalization (*D*, Figure 10) is apparent (Figure 9). Relative to the free dianions **27**, $\eta^5$-$Li^+$ complexation results in more equalized C−C distances in both **28** and in **29**; this is especially evident for the heavier metalloles (Figure 10).

The metallolyl cations **23** prefer planar $C_{2v}$ geometries (Figure 4). The four $\pi$-electrons increase the degree of C−C bond length alternation due to antiaromaticity for Si to Pb, but this increase is significantly larger in the

(28) The inversion barriers and the pyramidalities of silyl anions and amine ground states are related: (a) Damewood, J. R., Jr.; Hadad, C. M. *J. Phys. Chem.* **1988**, *92*, 33. (b) Stackhouse, J.; Baechler, R. D.; Mislow, K. *Tetrahedron Lett.* **1971**, *37*, 3437, 3441.

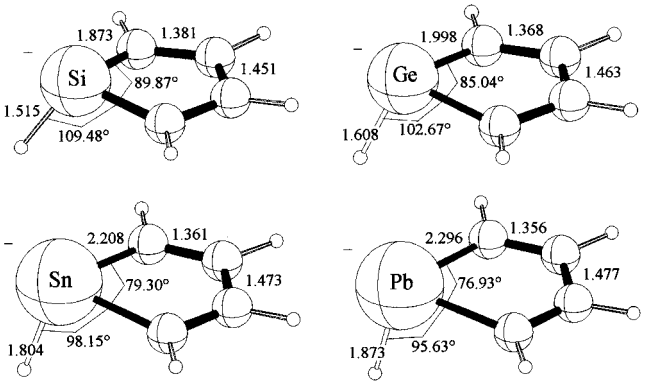


**Figure 2.** Optimized geometries (B3LYP/6-31+G* (C, H), /LanL2DZdp (E)) of metallolyl anions **21** ($C_s$). Bond distances are given in Å.

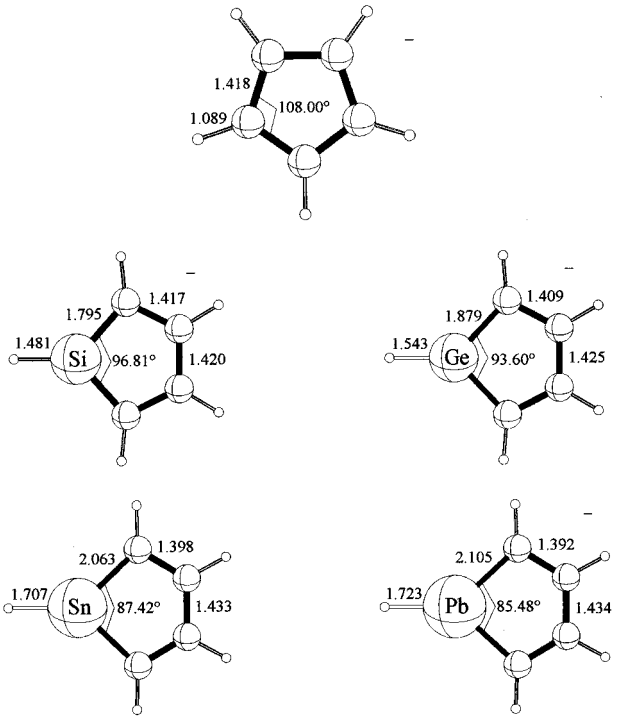


**Figure 3.** Optimized geometries (B3LYP/6-31+G* (C, H), /LanL2DZdp (E)) of planar metallolyl anions **22** ($C_{2v}$; **22-C**, $D_{5h}$). Bond distances are given in Å.

highly antiaromatic singlet **23-C**[29] (Figure 11). The singlet metallacyclopentadienylidenes **24-C**[30] to **24-Pb** show a dependence of *D* similar to that for **23** (Figure 11), due to a similar four-$\pi$-electron structure. The

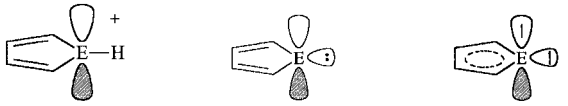

**23** ($^1A_1$, $C_{2v}$) **24** ($^1A_1$, $C_{2v}$) **25** ($^3B_1$, $C_{2v}$)

electron configurations in the $^3B_1$ triplets result in more equalized C−C lengths (lower *D* values) in all the **25** species (Figure 11). Triplet **25-C** is more stable than

(29) (a) Glukhovtsev, M. N.; Bach, R. D.; Laiter, S. *J. Phys. Chem.* **1996**, *100*, 10952. (b) Glukhovtsev, M. N.; Reindl, B.; Schleyer, P. v. R. *Mendeleev Commun.* **1993**, 100.

(30) For consistency, $C_{2v}$ geometries were employed for all metallolylidenes (C to Pb). For earlier computations on cyclopentadienylidene see: (a) Collins, C. L.; Davy, R. D.; Schaefer, H. F., III. *Chem. Phys. Lett.* **1990**, *171*, 259. (b) Bofill, J. M.; Bru, N.; Farràs, J.; Olivella, S.; Solé, A.; Vilarrasa, J. *J. Am. Chem. Soc.* **1988**, *110*, 3740.

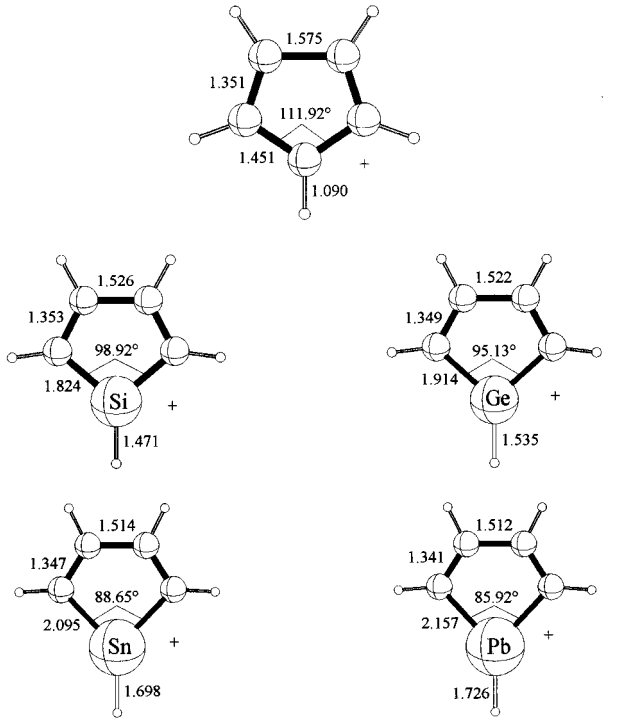


**Figure 4.** Optimized geometries (B3LYP/6-31+G* (C, H), /LanL2DZdp (E)) of metallolyl cations **23** ($C_{2v}$). Bond distances are given in Å.

singlet **24-C**, but the singlet structures **24** are lower in energy for Si to Pb (Table 4).

The isodesmic stabilization energies (ISE) of **21**−**23**, **26**, and **29** relative to the 1,1-dihydrometalloles **20** and acyclic reference compounds can be assessed by eq 1 (Tables 5−8).[31]

Evaluation of isodesmic stabilization energies (ISE):[31]

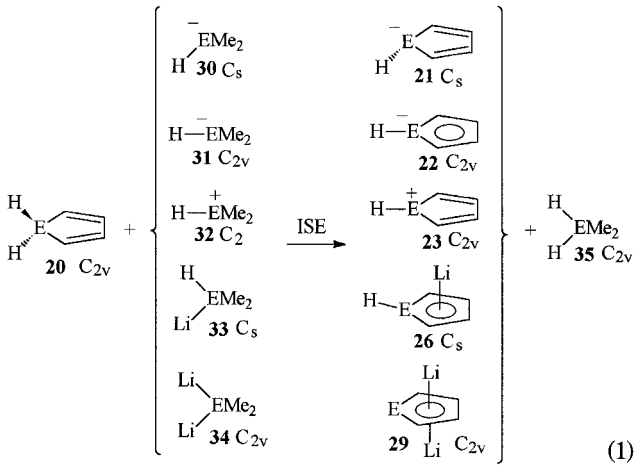


(1)

The ISEs of planar **22** are more negative than those of **21** with pyramidal heteroatoms (Figure 12); this indication of higher aromaticity is consistent with the degree of C−C bond length equalization (Figure 8). The stabilization in the lithium complexes **26** increases from **26-Si** to **26-Pb**; however, this is not due to a higher degree of aromaticity but is due to an increase in the stabilizing $Li^+-H^-$ interactions in **26-Ge** to **26-Pb** (apparent from short Li−H distances, Figure 5).[32] In accord with the C−C bond length equalization values (*D*) in Figure 11, the destabilization due to antiaromaticity (positive ISE) in **23** is decreased for **23-Si** to **23-Pb** relative to **23-C** (Figure 12). The ISE's of the dilithium metalloles **29-C** to **29-Pb** are the most negative and are remarkably constant for all group 14 species (Figure 12).

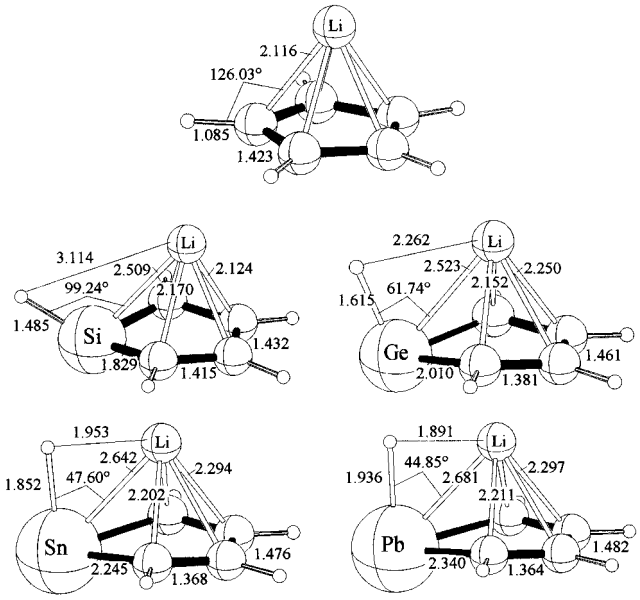


**Figure 5.** Optimized geometries (B3LYP/6-31+G* (C, H), /LanL2DZdp (E)) of lithium metallolides **26** ($C_s$; **26-C**, $C_{5v}$). Bond distances are given in Å.

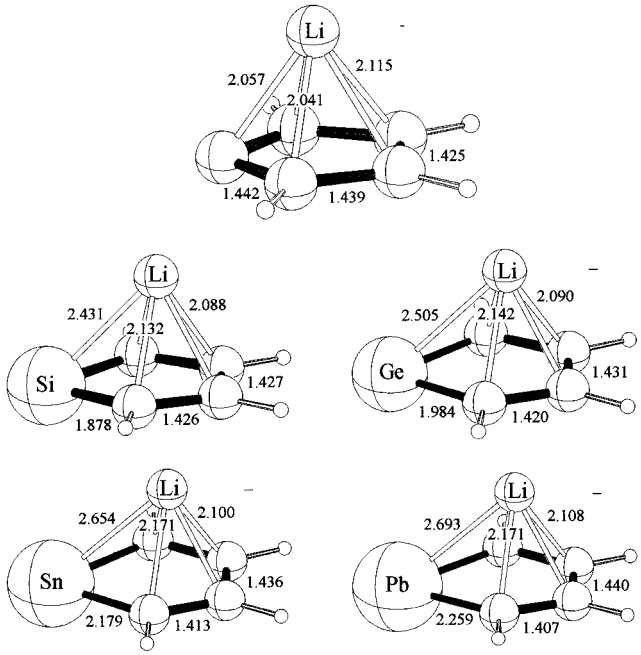


**Figure 6.** Optimized geometries (B3LYP/6-31+G* (C, H), /LanL2DZdp (E)) of lithium metallolyl anions **28** ($C_s$). Bond distances are given in Å.

**Magnetic Criteria.** Diamagnetic susceptibility exaltations Λ provide a measure of the degree of aromaticity.[33] The Λ value is defined as the difference between the diamagnetic susceptibility of the system

(31) Interactions between lithiums and methyl groups in **33** and **34** can result in more stable minimum structures with planar tetracoordinate E environments. For consistency, all **33** and **34** geometries were computed with tetrahedrally coordinated E's.

(32) For a discussion of the increase in aromaticity by $Li^+$ complexation see refs 13 and 18b.

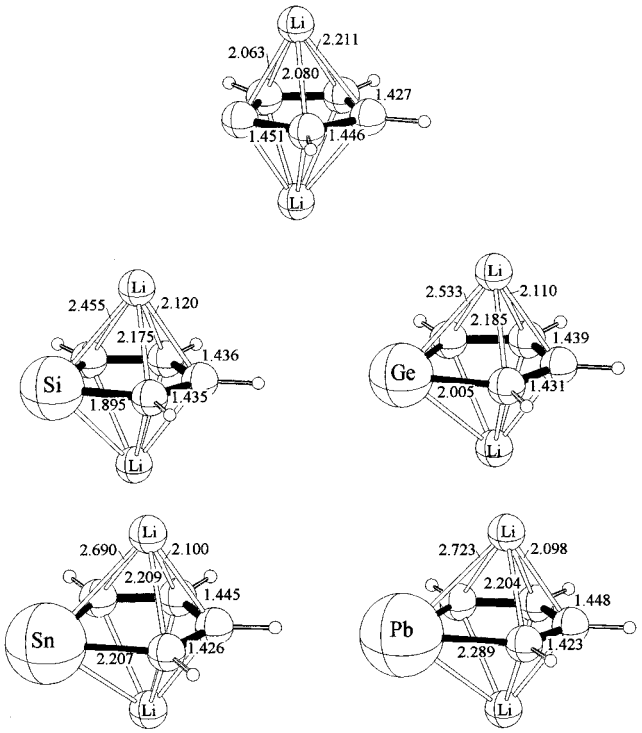


**Figure 7.** Optimized geometries (B3LYP/6-31+G* (C, H), /LanL2DZdp (E)) of dilithium metalloles **29** ($C_{2v}$). Bond distances are given in Å.

**Chart 1**

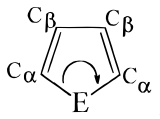


E = C to Pb

[a] The geometrical data for singlet **24** ($C_{2v}$), triplet **25** ($C_{2v}$), and $E^{2-}$ **27** ($C_{2v}$) are given in Table 1.

**Table 1. Bond Distances (Å) and Angles (deg) of Singlet $C_4H_4E$ (24, $C_{2v}$), Triplet $C_4H_4E$ (25, $C_{2v}$), and $C_4H_4E^{2-}$ (27, $C_{2v}$) (Chart 1)[a]**

| E | E−Cα | Cα−Cβ | Cβ−Cβ | Cα−E−Cα |
|---|---|---|---|---|
| singlet C | 1.511 | 1.343 | 1.532 | 102.34 |
| triplet C | 1.429 | 1.377 | 1.483 | 112.93 |
| $C^{2-}$ | 1.437 | 1.435 | 1.423 | 103.22 |
| singlet Si | 1.925 | 1.348 | 1.502 | 87.57 |
| triplet Si | 1.835 | 1.372 | 1.468 | 96.49 |
| $Si^{2-}$ | 1.880 | 1.407 | 1.430 | 88.03 |
| singlet Ge | 2.023 | 1.348 | 1.499 | 84.66 |
| triplet Ge | 1.835 | 1.366 | 1.470 | 92.91 |
| $Ge^{2-}$ | 1.994 | 1.394 | 1.440 | 84.34 |
| singlet Sn | 2.200 | 1.350 | 1.495 | 80.20 |
| triplet Sn | 2.125 | 1.360 | 1.474 | 86.52 |
| $Sn^{2-}$ | 2.198 | 1.379 | 1.453 | 79.06 |
| singlet Pb | 2.268 | 1.349 | 1.493 | 78.44 |
| triplet Pb | 2.208 | 1.353 | 1.477 | 84.10 |
| $Pb^{2-}$ | 2.281 | 1.371 | 1.460 | 76.93 |

[a] B3LYP/6-31+G* (C, H), /LanL2DZdp (E) optimized geometries.

under investigation ($\chi_M$) and the diamagnetic susceptibility for a hypothetical reference system without cyclic electron delocalization ($\chi_{M'}$): $\Lambda = \chi_M - \chi_{M'}$. We employed Scheme 2 for the calculation of $\chi_{M'}$ (Table 9).

Strongly negative (aromatic) Λ values are computed for the planar metallolyl anions **22** (Figure 13) and for the dilithium metalloles **29** (Figure 14). The increasing pyramidality at E from C to Pb both in **21** and in **26** gives rise to less negative Λ's (Figure 13). The highly

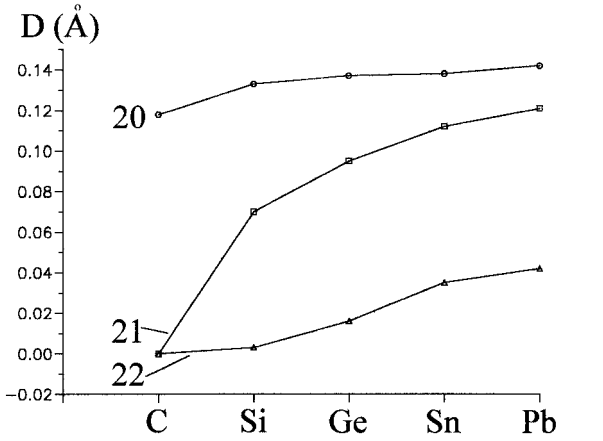


**Figure 8.** Bond length differences *D* of $C_\beta-C_\beta$ and $C_\alpha-C_\beta$ distances in the metallole rings of **20**−**22**.

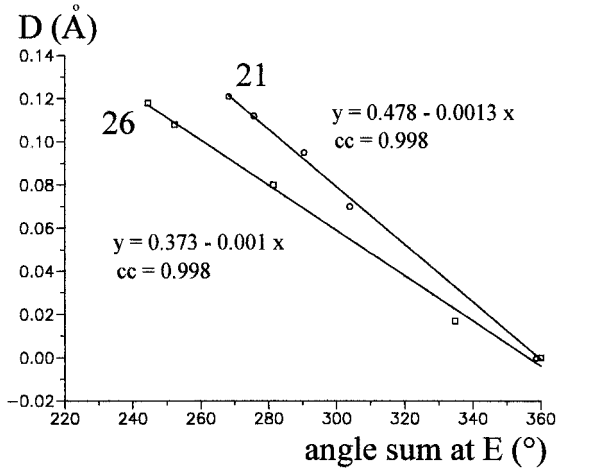


**Figure 9.** Correlation between the angle sums at E and the C−C bond lengths differences *D* of metallolyl anions **21** and their lithium complexes **26**.

**Table 2. Inversion Barriers of Metallolyl Anions (21, 22)[a]**

| | total energy (au)[a] | ZPE (kcal/mol)[b] | inversion barrier (kcal/mol)[c] |
|---|---|---|---|
| **22-C** ($D_{5h}$) | −193.534 78 | 49.33 (0) | 0.0 (−4.93) |
| **21-Si** ($C_s$) | −159.306 78 | 44.39 (0) | |
| **22-Si** ($C_{2v}$) | −159.297 06 | 44.12 (1) | 5.83 (−26.58) |
| **21-Ge** ($C_s$) | −159.188 44 | 43.44 (0) | |
| **22-Ge** ($C_{2v}$) | −159.166 38 | 43.32 (1) | 13.73 (−25.89) |
| **21-Sn** ($C_s$) | −158.788 82 | 42.45 (0) | |
| **22-Sn** ($C_{2v}$) | −158.747 99 | 42.46 (1) | 25.63 (−18.40) |
| **21-Pb** ($C_s$) | −158.867 45 | 41.71 (0) | |
| **22-Pb** ($C_{2v}$) | −158.807 82 | 41.98 (1) | 37.69 (−20.12) |

[a] B3LYP/6-31+G* (C, H), /LanL2DZdp (E) optimized geometries. [b] B3LYP zero-point energies; number of imaginary frequencies in parentheses. [c] Reduced inversion barriers relative to the corresponding $Me_2EH^-$ anions (see Table 3).

positive Λ value of **23-C** points to strong antiaromaticity, while the Λ's of the heavier metalloles **23-Sn** and **23-Pb** approach the lower values of **20** (Figure 14).

(33) (a) Dauben, H. J., Jr.; Wilson, J. D.; Laity, J. L. *J. Am. Chem. Soc.* **1968**, *90*, 811. (b) Dauben, H. J., Jr.; Wilson, J. D.; Laity, J. L. *J. Am. Chem. Soc.* **1969**, *91*, 1991. (c) Dauben, H. J., Jr.; Wilson, J. D.; Laity, J. L. In *Nonbenzenoid Aromatics*; Snyder, J. P., Ed.; Academic Press: New York, 1971; Vol. II, p 187 and references therein. For further applications of Λ as a criterion for aromaticity see refs 2, 13, 22 and: Simion, D. V.; Sorensen, T. S. *J. Am. Chem. Soc.* **1996**, *118*, 7345. Deviations among Λ values for identical systems are due to the use of different increment schemes to estimate $\chi_{M'}$ and different methods (e.g. IGLO or CSGT) for the susceptibility $\chi$ computations.

**Table 3. Inversion Barriers of $Me_2EH^-$ Series 30 ($C_s$) and 31 ($C_{2v}$)[a]**

| | total energy (au)[a] | ZPE (kcal/mol)[b] | inversion barrier (kcal/mol) |
|---|---|---|---|
| **30-C** ($C_s$) | −118.468 56 | 53.96 (0) | |
| **31-C** ($C_{2v}$) | −118.458 42 | 52.53 (1) | 4.93 |
| **30-Si** ($C_s$) | −84.320 00 | 49.52 (0) | |
| **31-Si** ($C_{2v}$) | −84.268 75 | 49.77 (1) | 32.41 |
| **30-Ge** ($C_s$) | −84.210 01 | 48.32 (0) | |
| **31-Ge** ($C_{2v}$) | −84.148 23 | 49.17 (1) | 39.62 |
| **30-Sn** ($C_s$) | −83.818 27 | 47.12 (0) | |
| **31-Sn** ($C_{2v}$) | −83.749 81 | 48.19 (1) | 44.03 |
| **30-Pb** ($C_s$) | −83.899 12 | 46.25 (0) | |
| **31-Pb** ($C_{2v}$) | −83.809 68 | 47.94 (1) | 57.81 |

[a] B3LYP/6-31+G* (C, H), /LanL2DZdp (E) optimized geometries. [b] B3LYP zero-point energies; number of imaginary frequencies in parentheses.

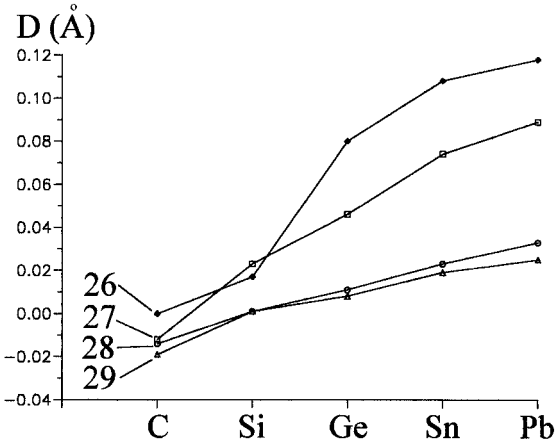


**Figure 10.** Bond length differences $D$ of $C_\beta-C_\beta$ and $C_\alpha-C_\beta$ distances in the metallole rings of **26**−**29**.

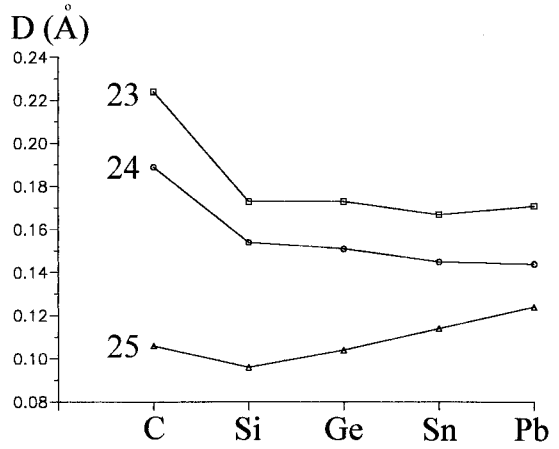


**Figure 11.** Bond length differences $D$ of $C_\beta-C_\beta$ and $C_\alpha-C_\beta$ distances in the metallole rings of **23**−**25**.

Nucleus-independent chemical shifts (NICS) computed at ring centers (nonweighted mean of the heavy-atom coordinates)[34] are efficient probes for dia- and paratropic ring currents, associated with aromaticity and antiaromaticity, respectively.[35] The planar metallolyl anions **22** exhibit more negative NICS's (Table 10) than the anions in the nonplanar geometries **21-Si** to **21-Pb** (Figure 15). This is consistent with larger ring currents and higher aromaticity in the planar species. The lithium metallolides **26** and the free anions **21** show similar trends from C to Pb again, due to the increased pyramidality at E (Figure 15). The large positive (antiaromatic) NICS of **23-C** (+49.2) is exceptional; the NICS in **23-Si** (+18.6) is much smaller and decreases down the group to **23-Pb** (+5.2, Figure 16). The NICS's of **20-C** to **20-Pb** are displaced to more negative values in **29-C** to **29-Pb**, reflecting the higher aromatic degree of the dilithium species (Figure 16). Consistently, the $^7$Li shielding[18] decreases more strongly from C to Pb in **26** than in **29** (Figure 17).

(34) The different NICS positions in planar and nonplanar molecules give rise to NICS values, which are not comparable directly.

(35) NICS is based on computed absolute magnetic shieldings with the signs reversed to conform to the experimental NMR conventions: Schleyer, P. v. R.; Maerker, C.; Dransfeld, A.; Jiao, H.; Hommes, N. J. R. v. E. *J. Am. Chem. Soc.* **1996**, *118*, 6317.

**Table 4. Singlet−Triplet Splitting in Metallolylidenes 24 and 25[a]**

| | total energy (au)[a] | ZPE (kcal/mol)[b] | singlet **24** vs triplet **25** (kcal/mol) |
|---|---|---|---|
| **24-C** ($^1A_1$, $C_{2v}$) | −192.746 12 | 41.55 (1) | |
| **25-C** ($^3B_1$, $C_{2v}$) | −192.784 81 | 42.09 (0) | +23.74 |
| **24-Si** ($^1A_1$, $C_{2v}$) | −158.623 84 | 40.04 (1) | |
| **25-Si** ($^3B_1$, $C_{2v}$) | −158.605 16 | 40.53 (0) | −12.21 |
| **24-Ge** ($^1A_1$, $C_{2v}$) | −158.525 00 | 39.64 (0) | |
| **25-Ge** ($^3B_1$, $C_{2v}$) | −158.491 21 | 39.79 (0) | −20.79 |
| **24-Sn** ($^1A_1$, $C_{2v}$) | −158.138 17 | 39.35 (0) | |
| **25-Sn** ($^3B_1$, $C_{2v}$) | −158.094 99 | 39.19 (0) | −26.94 |
| **24-Pb** ($^1A_1$, $C_{2v}$) | −158.230 35 | 39.07 (0) | |
| **25-Pb** ($^3B_1$, $C_{2v}$) | −158.173 81 | 38.04 (0) | −34.45 |

[a] B3LYP/6-31+G* (C, H), /LanL2DZdp (E) optimized geometries. [b] B3LYP zero-point energies and number of imaginary frequencies in parentheses.

**Table 5. Isodesmic Stabilization Energies (ISE; Eq 1) of Nonplanar (21) and Planar (22) Metallolyl Anions[a]**

| | total energy (au)[a] | ZPE (kcal/mol)[b] | ISE (kcal/mol)[c] |
|---|---|---|---|
| **20-C** ($C_{2v}$) | −194.110 33 | 58.13 (0) | −63.16 (for **30**−**C**, pyramidal) |
| **35-C** ($C_{2v}$) | −119.148 44 | 65.07 (0) | −68.09 (for **31**−**C**, planar) |
| **20-Si** ($C_{2v}$) | −159.891 91 | 51.59 (0) | −23.10 (**21**−**Si**) |
| **35-Si** ($C_{2v}$) | −84.942 29 | 56.94 (0) | −49.68 (**22**−**Si**) |
| **20-Ge** ($C_{2v}$) | −159.759 40 | 50.32 (0) | −18.00 (**21**−**Ge**) |
| **35-Ge** ($C_{2v}$) | −84.810 33 | 55.62 (0) | −43.90 (**22**−**Ge**) |
| **20-Sn** ($C_{2v}$) | −159.340 87 | 48.65 (0) | −13.80 (**21**−**Sn**) |
| **35-Sn** ($C_{2v}$) | −84.392 85 | 53.66 (0) | −32.20 (**22**−**Sn**) |
| **20-Pb** ($C_{2v}$) | −159.396 02 | 47.95 (0) | −11.90 (**21**−**Pb**) |
| **35-Pb** ($C_{2v}$) | −84.447 57 | 53.06 (0) | −32.03 (**22**−**Pb**) |

[a] B3LYP/6-31+G* (C, H), /LanL2DZdp (E) optimized geometries. [b] B3LYP zero-point energies; number of imaginary frequencies in parentheses. [c] Energies of **21**, **22**, **30**, and **31** are given in Tables 2 and 3.

**Table 6. Isodesmic Stabilization Energies (ISE; Eq 1) of Metallolyl Cations 23[a]**

| | total energy (au)[a] | ZPE (kcal/mol)[b] | ISE (kcal/mol)[c] |
|---|---|---|---|
| **32-C** ($C_2$) | −118.212 70 | 55.61 (0) | |
| **23-C** ($C_{2v}$) | −193.155 50 | 50.05 (0) | 13.36 |
| **32-Si** ($C_2$) | −84.036 63 | 50.77 (0) | |
| **23-Si** ($C_{2v}$) | −158.978 27 | 46.21 (0) | 5.80 |
| **32-Ge** ($C_2$) | −83.918 78 | 50.14 (0) | |
| **23-Ge** ($C_{2v}$) | −158.859 33 | 45.29 (0) | 5.80 |
| **32-Sn** ($C_2$) | −83.519 58 | 49.18 (0) | |
| **23-Sn** ($C_{2v}$) | −158.459 00 | 44.28 (0) | 5.51 |
| **32-Pb** ($C_2$) | −83.591 07 | 48.93 (0) | |
| **23-Pb** ($C_{2v}$) | −158.530 40 | 43.72 (0) | 5.62 |

[a] B3LYP/6-31+G* (C, H), /LanL2DZdp (E) optimized geometries. [b] B3LYP zero-point energies; number of imaginary frequencies in parentheses. [c] Energies of **20** and **35** are given in Table 5.

## Conclusions

Structural (the degree of C−C bond length equalization, D), energetic (ISE), and magnetic (Λ, NICS)

**Scheme 2. Increment Scheme for the Evaluation of the Diamagnetic Susceptibilities $\chi_M'$ for Metallole Reference Systems[a]**

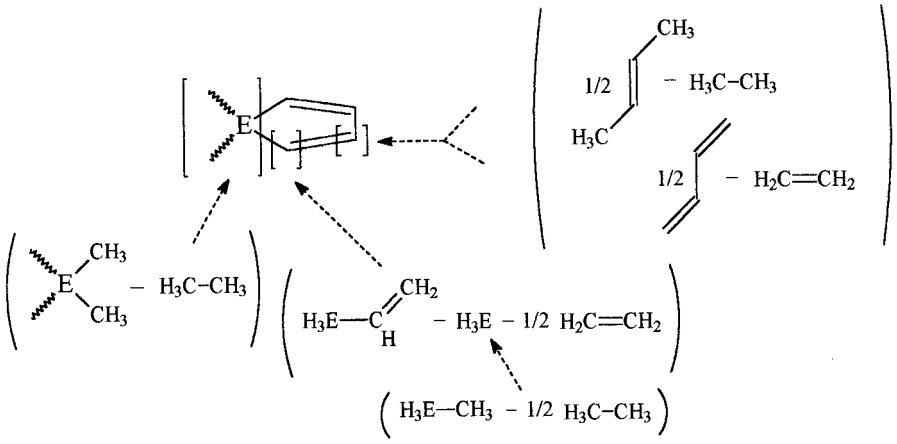


[a] The magnetic susceptibility of $C_\alpha H$ groups is obtained from $\chi(H_3E{-}CH{=}CH_2)$ minus $\chi(H_3E)$, minus $^1/_2\chi(H_2C{=}CH_2)$. The $\chi(H_3E)$ magnetic susceptibility is obtained from $\chi(H_3E{-}CH_3)$ minus $^1/_2\chi(H_3C{-}CH_3)$. Similarly, the magnetic susceptibility of $C_\beta H$ groups is based on the mean values for dimethylethene and butadiene moieties. The magnetic susceptibilities of the element functionalities (e.g. $H_2E$) are obtained from $\chi(H_2E(CH_3)_2)$ minus $\chi(H_3C{-}CH_3)$.

**Table 7. Isodesmic Stabilization Energies (ISE; Eq 1) of Lithium Metallolides 26[a]**

| | total energy (au)[a] | ZPE (kcal/mol)[b] | ISE (kcal/mol)[c] |
|---|---|---|---|
| **33-C** ($C_s$) | −126.019 91 | 57.16 (0) | |
| **26-C** ($C_s$) | −201.085 81 | 52.77 (0) | −62.72 |
| **33-Si** ($C_s$) | −91.844 96 | 51.88 (0) | |
| **26-Si** ($C_s$) | −166.842 73 | 47.23 (0) | −29.51 |
| **33-Ge** ($C_s$) | −91.725 15 | 50.78 (0) | |
| **26-Ge** ($C_s$) | −166.720 78 | 45.87 (0) | −28.83 |
| **33-Sn** ($C_s$) | −91.321 26 | 49.45 (0) | |
| **26-Sn** ($C_s$) | −166.320 09 | 44.95 (0) | −31.37 |
| **33-Pb** ($C_s$) | −91.388 83 | 48.90 (0) | |
| **26-Pb** ($C_s$) | −166.405 62 | 44.40 (0) | −42.27 |

[a] B3LYP/6-31+G* (C, H), /LanL2DZdp (E) optimized geometries.[31] [b] B3LYP zero-point energies; number of imaginary frequencies in parentheses. [c] Energies of **20** and **35** are given in Table 5.

**Table 8. Isodesmic Stabilization Energies (ISE; Eq 1) of Dilithium Metalloles 29[a]**

| | total energy (au)[a] | ZPE (kcal/mol)[b] | ISE (kcal/mol)[c] |
|---|---|---|---|
| **34-C** ($C_{2v}$) | −132.888 12 | 49.46 (1) | |
| **29-C** ($C_{2v}$) | −207.976 38 | 46.25 (0) | −75.57 |
| **34-Si** ($C_{2v}$) | −98.742 52 | 47.33 (0) | |
| **29-Si** ($C_{2v}$) | −173.807 26 | 43.85 (0) | −70.37 |
| **34-Ge** ($C_{2v}$) | −98.633 11 | 46.58 (0) | |
| **29-Ge** ($C_{2v}$) | −173.697 34 | 43.09 (0) | −70.45 |
| **34-Sn** ($C_{2v}$) | −98.241 29 | 45.85 (0) | |
| **29-Sn** ($C_{2v}$) | −173.297 03 | 42.58 (0) | −65.86 |
| **34-Pb** ($C_{2v}$) | −98.317 71 | 45.37 (0) | |
| **29-Pb** ($C_{2v}$) | −173.383 42 | 42.24 (0) | −71.60 |

[a] B3LYP/6-31+G* (C, H), /LanL2DZdp (E) optimized geometries.[31] [b] B3LYP zero point energies; number of imaginary frequencies in parentheses. [c] Energies of **20** and **35** are given in Table 5.

assessments of the aromaticity and antiaromaticity in various group 14 metalloles result in the following general conclusions.

(1) The aromaticity of the metallolyl anions $C_4H_4EH^-$ (**21**, $C_s$) increases with decreasing pyramidality at the heteroatom E (i.e. from Pb to C) and is significantly higher for the planar $C_{2v}$ geometries **22**. Except for $C_5H_5^-$, the planar species are transition structures for inversion. The barriers decrease from Pb to C.

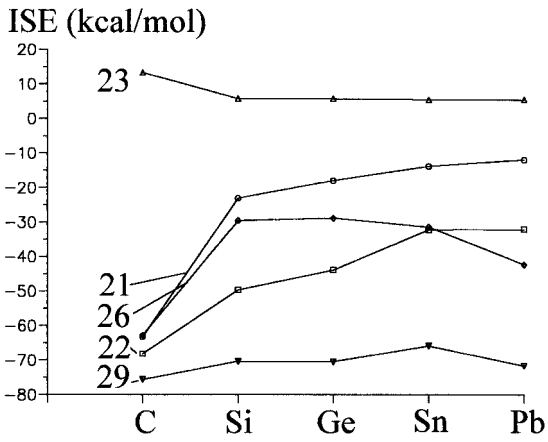


**Figure 12.** Isodesmic stabilization energies (ISE) according to eq 1.

**Table 9. Magnetic Susceptibilities $\chi$ and Exaltations $\Lambda$ (ppm cgs)[a]**

| | | **20** | **21** | **22** | **23** | **26** | **29** |
|---|---|---|---|---|---|---|---|
| C | $\chi_M$ | −42.38 | −54.45 | −54.45 | −0.11 | −55.05 | −54.79 |
| | $\chi_{M'}$ | −38.21 | −36.43 | −36.43 | −28.32 | −38.12 | −30.09 |
| | $\Lambda$ | −4.17 | −18.02 | −18.02 | +28.21 | −16.93 | −23.89 |
| Si | $\chi_M$ | −41.42 | −55.48 | −62.88 | −22.79 | −57.56 | −66.70 |
| | $\chi_{M'}$ | −37.80 | −40.87 | −40.87 | −29.20 | −41.11 | −43.03 |
| | $\Lambda$ | −3.62 | −14.61 | −22.01 | +6.41 | −16.45 | −23.67 |
| Ge | $\chi_M$ | −42.14 | −52.33 | −63.59 | −25.26 | −54.82 | −65.92 |
| | $\chi_{M'}$ | −38.65 | −41.50 | −41.50 | −28.65 | −42.29 | −45.21 |
| | $\Lambda$ | −3.49 | −10.83 | −22.09 | +3.39 | −12.53 | −20.71 |
| Sn | $\chi_M$ | −43.05 | −51.56 | −65.22 | −29.34 | −53.10 | −69.00 |
| | $\chi_{M'}$ | −39.78 | −43.94 | −43.94 | −28.82 | −44.54 | −49.89 |
| | L | −3.27 | −7.62 | −21.28 | −0.52 | −8.56 | −19.11 |
| Pb | $\chi_M$ | −44.11 | −49.05 | −64.50 | −31.19 | −50.23 | −65.26 |
| | $\chi_{M'}$ | −40.37 | −43.60 | −43.60 | −27.40 | −44.83 | −50.30 |
| | L | −3.74 | −5.45 | −20.90 | −3.79 | −5.40 | −14.96 |

[a] CSGT-SCF/6-311++G** (C, H), /6-31G* (Li), /LanL2DZdp (E) NMR computations; //B3LYP/6-31+G* (C, H), /6-31G* (Li), /LanL2DZdp (E) optimized geometries.

(2) The antiaromaticity in the singlet cyclopentadienyl cation **23-C** is strongly reduced in the heavier metalloles and is about constant (*D*) or decreases only slightly (ISE, $\Lambda$, NICS) from **23-Si** to **23-Pb**.

(3) Increased pyramidality at E decreases the aromaticity in lithium metallolides $C_4H_4EHLi$ (**26**, $C_s$) to a

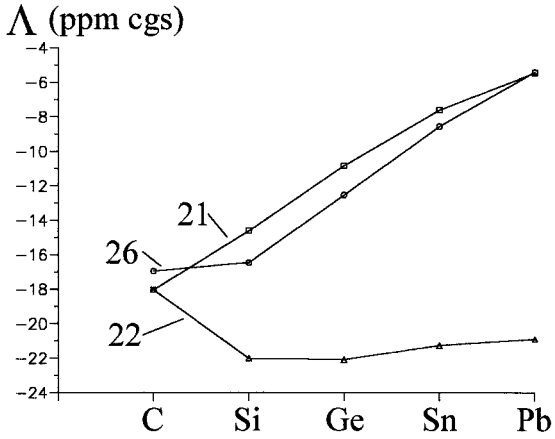


**Figure 13.** Magnetic susceptibility exaltations Λ of metallolyl anions **21** and **22** and their $Li^+$ complexes **26**.

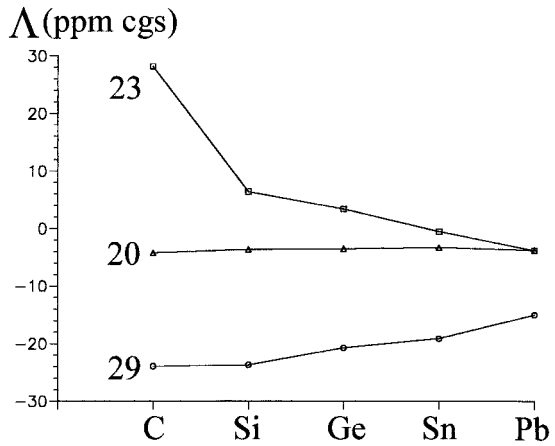


**Figure 14.** Magnetic susceptibility exaltations Λ of 1,1-dihydrometalloles **20**, of metallolyl cations **23**, and of dilithium metalloles **29**.

**Table 10. Nucleus-Independent Chemical Shifts (NICS's; ppm)[a] and (in Parentheses) $\delta(^7Li)$ Values[b]**

| | 20 | 21 | 22 | 23 | 26 | 29 |
|---|---|---|---|---|---|---|
| C | −3.22 | −14.32 | −14.32 | +49.22 | −17.20 (−9.0) | −16.21 (−9.2) |
| Si | +6.15 | −3.76 | −10.60 | +18.62 | −0.96 (−5.3) | −0.53 (−9.0) |
| Ge | +4.12 | −2.71 | −11.78 | +13.70 | +0.46 (−3.1) | −5.41 (−8.1) |
| Sn | +3.52 | −1.65 | −10.76 | +9.27 | +1.49 (−1.8) | −6.88 (−6.7) |
| Pb | +0.52 | −2.22 | −12.97 | +5.23 | +0.08 (−1.6) | −10.04 (−6.0) |

[a] GIAO-SCF/6-31+G* (C, H), /6-31G* (Li) [/6-311+G* for ($\delta$(Li))], /LanL2DZdp (E) NMR computations on B3LYP/6-31+G* (C, H), /6-31G* (Li), /LanL2DZdp (E) optimized geometries. The reversed signs of the absolute magnetic shieldings (computed at ring centers, i.e. the nonweighted mean of the heavy-atom coordinates) were used as the NICS values. [b] $Li^+(H_2O)_4$, $\sigma$(Li) = 91.9.

similar degree as in **21**. However, Li−H interactions between the $\eta^5$-bound Li's and the hydrogens of the E−H bonds stabilize significantly the heavier metalloles **26-Sn** and **26-Pb**.

(4) The dilithium metalloles **29** are the most aromatic among all these species, even more than the dianions. This degree of aromaticity is remarkably constant for the metallole dianions (or the $Li^+$ complexes) down group 14.

Generally, both the aromaticity and the antiaromaticity of heavier group 14 metalloles are less than those of their carbon congeners. The increasing tendency toward pyramidalization at heteroatoms in the trivalent anionic species, and *not* an inherent 2p−3p overlap problem,[4] results in decreased aromaticity of the heavier metallolyl anions **21**. However, this pyramidalization bias is not present in the metallole dianions and their lithiated derivatives, and highly delocalized aromatic structures result.

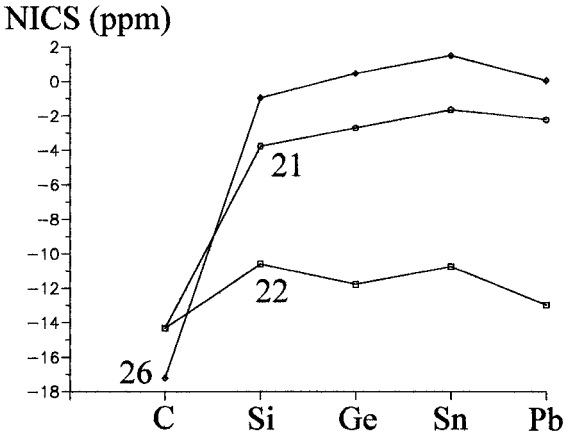


**Figure 15.** Nucleus-independent chemical shifts (NICS's) at ring centers of metallolyl anions **21** and **22** and their $Li^+$ complexes **26**.

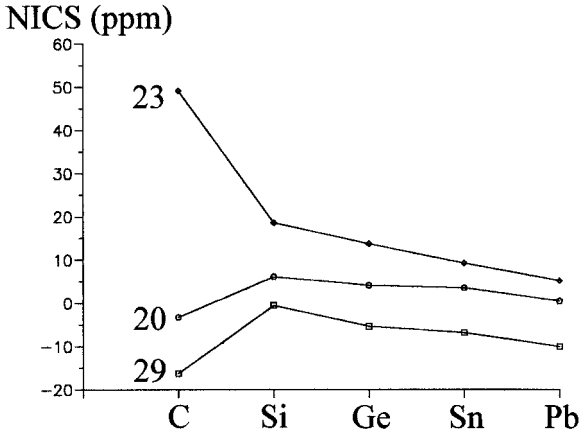


**Figure 16.** Nucleus-independent chemical shifts (NICS's) at ring centers of 1,1-dihydrometalloles **20**, of metallolyl cations **23**, and of dilithium metalloles **29**.

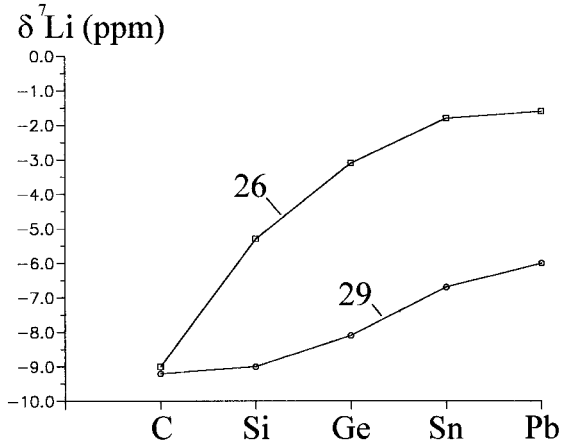


**Figure 17.** The $\delta(^7Li)$ values (vs $Li^+(H_2O)_4$, $\sigma$(Li) = 91.9) of lithium metallolides **26** and of dilithium metalloles **29**.

## Computational Details

All geometries were optimized in the symmetries given using the gradient techniques implemented in GAUSSIAN 94[36] with Becke's three-parameter hybrid exchange functional incorporating the Lee−Yang−Parr correlation functional

(Becke3LYP).[37] The 6-31+G* and 6-311++G** basis sets were used for C and H. For Si, Ge, Sn, and Pb four-valence-electrons effective core potentials of Wadt and Hay (relativistic for Pb) and the LanL2DZ basis sets,[38] augmented with s- and p- diffuse basis functions[39] and with d-polarization functions[40] (LanL2DZdp), were employed. The character of the stationary points and the zero-point energy corrections were obtained from analytical and, for the pseudopotential computations of the Si to Pb systems, from numerical frequency calculations. The magnetic susceptibility exaltations were computed with the CSGT (continuous set of gauge transformations) method.[41] Absolute chemical shieldings (the reversed signs give NICS values)[35] were computed with the GIAO (gauge-including atomic orbitals) method.[42]

**Acknowledgment.** This work was supported by the Fonds der Chemischen Industrie (also through a scholarship to B.G.), the Stiftung Volkswagenwerk, the Convex Computer Corp., and the Deutsche Forschungsgemeinschaft. We thank Prof. T. D. Tilley (Berkeley) for a preprint of ref 16 and for his high interest.

**Supporting Information Available:** A table giving computed magnetic susceptibilities (1 page). Ordering information is given on any current masthead page.

OM960994V

(36) Gaussian 94, Revision C.3: Frisch, M. J.; Trucks, G. W.; Schlegel, H. B.; Gill, P. M. W.; Johnson, B. G.; Robb, M. A.; Cheeseman, J. R.; Keith, T.; Petersson, G. A.; Montgomery, J. A.; Raghavachari, K.; Al-Laham, M. A.; Zakrzewski, V. G.; Ortiz, J. V.; Foresman, J. B.; Cioslowski, J.; Stefanov, B. B.; Nanayakkara, A.; Challacombe, M.; Peng, C. Y.; Ayala, P. Y.; Chen, W.; Wong, M. W.; Andres, J. L.; Replogle, E. S.; Gomperts, R.; Martin, R. L.; Fox, D. J.; Binkley, J. S.; Defrees, D. J.; Baker, J.; Stewart, J. P.; Head-Gordon, M.; Gonzalez, C.; Pople, J. A. Gaussian, Inc., Pittsburgh, PA, 1995.

(37) (a) Becke, A. D. *J. Chem. Phys.* **1993**, *98*, 5648. (b) Lee, C.; Yang, W.; Parr, R. G. *Phys. Rev. B* **1988**, *37*, 785.

(38) Hay, P. J.; Wadt, W. R. *J. Chem. Phys.* **1985**, *82*, 299.

(39) Clark, T.; Chadrasekhar, J.; Spitznagel, G. W.; Schleyer, P. v. R. *J. Comput. Chem.* **1983**, *4*, 294. The diffuse s and p function exponents were obtained by multiplying the outermost functions of the LanL2DZ basis by 0.25.

(40) Huzinaga, S. *Gaussian Basis Sets for Molecular Calculations*; Elsevier: Amsterdam, 1984.

(41) (a) Keith, T. A.; Bader, R. F. W. *Chem. Phys. Lett.* **1993**, *210*, 223. (b) Keith, T. A.; Bader, R. F. W. *Chem. Phys. Lett.* **1992**, *194*, 1.

(42) (a) Wolinski, K.; Hilton, F. J.; Pulay, P. *J. Am. Chem. Soc.* **1990**, *112*, 8251. (b) Dodds, J. L.; McWeeney, R., Sadlej, A. J. *Mol. Phys.* **1980**, *41*, 1419. (c) Ditchfield, R. *Mol. Phys.* **1974**, *27*, 789. (d) McWeeny, R. *Phys. Rev.* **1962**, *126*, 1028. (e) London, F. *J. Phys. Radium* **1937**, *8*, 397.